CHEMICAL ENGINEERING TRANSACTIONS
VOL. 57, 2017
A publication of AIDIC
The Italian Association of Chemical Engineering
Online at www.aidic.it/cet
Guest Editors: Sauro Pierucci, Jiří Jaromír Klemeš, Laura Piazza, Serafim Bakalis

ISBN 978-88-95608- 48-8; **ISSN** 2283-9216

CFD Simulation of Natural Convective Flow in Pressurized Tanks Exposed to Fire

Andrea Rum, Gabriele Landucci*, Chiara Galletti, Leonardo Tognotti

Dipartimento di Ingegneria Civile e Industriale, Università di Pisa, Largo Lucio Lazzarino 2, 56126 Pisa, Italy
gabriele.landucci@unipi.it

Computational Fluid Dynamics (CFD) is a consolidated tool to support industrial projects development and was recently adopted in the framework of consequence assessment and safety analyses. In the present study, a CFD model of pressurized vessels exposed to an accidental fire was developed, with the aim to determine the transient behavior of the stored fluid during the heat-up. An integral model for consequence assessment was adopted in order to set advanced boundary conditions to the CFD model. The results of CFD simulations allowed predicting temperature and velocity of both liquid and vapor phases, as well as the complex recirculation phenomena induced by natural convection. This allowed determining the pressurization rate in the fired tank, thus obtaining key indications for the evaluation of the residual mechanical resistance.

1. Introduction

Severe fires, mainly due to the ignition of accidental releases, may affect process equipment or transport vessels leading to cascading events with catastrophic consequences (Necci et al., 2015). In the literature, several small and medium scale tests were carried out in order to investigate this type of accident chain and to provide indications on the behaviour of pressurized tanks exposed to fire (Moodie, 1988). Due to safety and economic reasons, a limited number of large scale tests is available (Birk, 2012). Therefore, the use of advanced computer models able to reproduce the heat-up of a vessel engulfed in flames or exposed to distant source radiation may constitute a sound tool to provide information for the emergency response and to set-up mitigation measures (Argenti et al., 2014).

In the present study, a Computational Fluid Dynamics (CFD) model was developed for pressurized vessels exposed to accidental fires, aimed at determining the transient behaviour of the stored fluid during the heat-up. As evidenced by experimental works (Birk and Cunningham, 1996), a key issue in modelling this system is the prediction of the stratification of the inner fluid during the heat-up process. The stratification is due to a buoyancy driven flow, caused by the more rapid temperature increase of the liquid in contact with the vessel walls heated by the fire with respect to the bulk fluid, as shown in recent studies for liquid (D'Aulisa et al., 2014a) and gas (D'Aulisa et al., 2014b) tanks. This process has a direct influence on the pressurization rate of the vessel, and thus it affects the time to failure, e.g. the lapse of time between the start of the fire and the eventual vessel rupture (Moodie, 1988).

A CFD model of the liquid and vapor phases in a two-dimensional circular geometry representing a cross-section of a large-scale cylindrical pressurised vessel was developed. Different filling level values and complex heat exposure conditions were simulated in a specific test case of industrial interest, in order to exemplify the potentialities of the present simulation approach.

2. Description of a test case

An industrial area in which atmospheric and pressurized tanks are installed is considered for the test case. An overview of the facility is shown in Figure 1, together with the features of the vessels involved in the test case (e.g., the atmospheric tank V1 and the pressurized tank V2). It is assumed that a failure in V1, storing crude oil, leads to a pool fire in the catch basin affecting the neighbouring tank V2, storing propane.

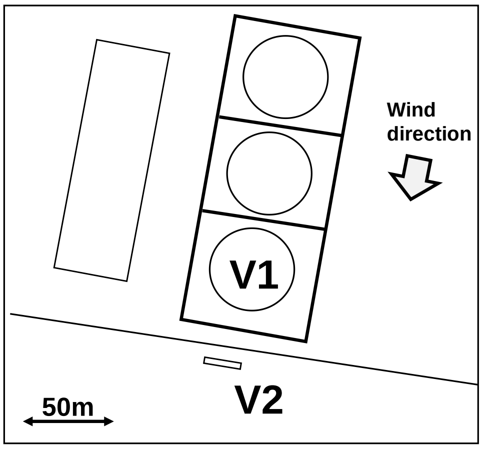

Item	Vessels features	
	V1	V2
Nominal diameter (m)	42	3.2
Nominal height/length (m)	3.6	19.4
Maximum wall thickness (mm)	11.3	27
Design pressure (barg)	0.02	17
Nominal volume (m^3)	5000	200
Stored fluid	Crude oil	Propane
Filling ratio (-)	0.7	0.9; 0.7
Inventory (t)	3000	94; 73
Area of the catch basin (m^2)	3575	Not relevant

Figure 1: Layout considered for the analysis of the test case and features of the vessels.

The consequences of the pool were evaluated using conventional literature integral models based on surface emissive power approximation (Van Den Bosh and Weterings, 2005). A single set of meteorological parameters was used to calculate the consequences of the pool fire, in particular considering uniform wind distribution (see Figure 1), blowing at 5 m/s in stability class D. Pool fire simulation allowed gathering non-uniform boundary conditions for the analysis of the heat-up of target V2 through the CFD model, thus providing an example of coupling of different kinds of models. The simulation set up is described in Section 3.

3. Numerical model

3.1 Computational Domain and grid

Since the storage tank has a length much larger than its diameter, a 2-dimensional (2D) domain corresponding to a cross section of the tank was chosen. An O-grid was generated with the ICEM software, by ANSYS Inc. and, hence, it is block structured. Such grid is refined near the walls. The number of cells is 268k; such high cell number (especially considering that the grid is 2D) is required to capture the liquid level rise due to the temperature increase in the storage tank.

3.2 Physical model

The physical model was solved with Fluent v. 15 by ANSYS Inc. and is based on the Volume of Fluid (VOF), that assumes that each control volume contains just one phase or the interface. This is determined by the volume fraction α_L of, say, the liquid phase, identifying three cases: 1) for $\alpha_L = 0$ the cell is full of vapor; 2) for $\alpha_L = 1$ the cell is full of liquid; 3) for $0<\alpha_L<1$ the cell contains the vapor-liquid interface.
Since the flow is turbulent, the equations that are solved are continuity, momentum and energy equations:

$$\frac{\partial \rho}{\partial t} + \nabla \cdot (\rho \mathbf{U}) = 0$$
$$\frac{\partial (\rho \mathbf{U})}{\partial t} + \nabla \cdot (\rho \mathbf{U}\mathbf{U}) = -\nabla P + \nabla \cdot (\mu + \mu_T)\left(\nabla \mathbf{U} + \nabla \mathbf{U}^T\right) + \mathbf{F} \tag{1}$$
$$\frac{\partial (\rho c_p T)}{\partial t} + \nabla \cdot \left[\mathbf{U}\left(\rho c_p T + P\right)\right] = \nabla \cdot \left[\left(\kappa + \frac{c_p \mu_T}{Pr_T}\right)\nabla T\right] + S_h$$

where ***U***, *T* and *P* are the mean velocity vector, temperature and pressure, respectively, and the superscript T indicates the transpose of a tensor; μ_T is the turbulent viscosity, determined through the standard *k-ε* turbulence model. In particular, such turbulence model was found to predict very well the heat-up in a pressurized tank uniformly exposed to a pool fire, providing a very good agreement with experimental data on temperature and pressure (D'Aulisa et al., 2014b). Pr_T is the turbulent Prandtl number which is equal to 0.85. The properties (density, specific heat and thermal conductivity) appearing in the transport equations are those of the phase present in each control volume and hence:

$$\rho = \alpha_L \rho_L + (1 - \alpha_L)\,\rho_V \qquad c_p = \alpha_L c_{pL} + (1 - \alpha_L)\,c_{pV} \qquad \kappa = \alpha_L \kappa_L + (1 - \alpha_L)\,\kappa_V \tag{2}$$

The liquid was modelled as incompressible, even though its density was allowed to vary with temperature in the body force term of the momentum equation using the Boussinesq model. The effect of surface tension was neglected as the estimated Eotvos number was much larger than 1.

The vapour-liquid interface was tracked by solving a volume fraction continuity equation for the liquid phase:

$$\frac{1}{\rho_L}\frac{\partial(\alpha_L\rho_L)}{\partial t} + \nabla\cdot(\alpha_L\rho_L\mathbf{U}) = S_{\alpha_L} + (\dot{m}_{VL} - \dot{m}_{LV}) \quad (3)$$

where $S_{\alpha L}$ is the rate of increase of liquid volume fraction due to external liquid mass source term, whereas $\dot{m}_{VL}$ and $\dot{m}_{LV}$ represent mass transfer due to condensation and evaporation, respectively, determined using the Lee Model (Lee, 1980). The model assumes that the mass is transferred at a constant pressure and a quasi-thermo-equilibrium state.

The fluid stored in the vessel exposed to the fire is pure propane; the saturation temperature and latent heat of vaporization were expressed as a function of the absolute pressure P, through a polynomial as described in (Landucci et al., 2016), whereas the vapour density was estimated using the Peng Robinson equation.

The pressure-based solver with an implicit time advancement of Fluent v. 16, by Ansys Inc., was employed. The Courant number was lower than 5. A first order upwind discretization with the SIMPLE algorithm scheme for the pressure-velocity coupling was applied for all equations. Normalized residuals for all equations were typically well below 10^{-6}. One hour of CPU time was needed to cover 1 s of real time when run on 32 threads. Simulations were run to cover the time up to tank pressurization corresponding to the set pressure of the release valve.

3.3 Boundary conditions

A non-uniform heat flux conditions was set at the walls through a bespoke subroutine describing the variation of incident flux with the angular coordinate of the tank wall as calculated from the integral model (see Figure 2). Two different initial liquid levels were considered for vessel V2, i.e. 90% (case “a”) and 70% (case “b”). Detailed transient temperature behaviour in the liquid phase is shown in Section 4 for the three spots represented in Figure 2 (T1, T2 and T3).

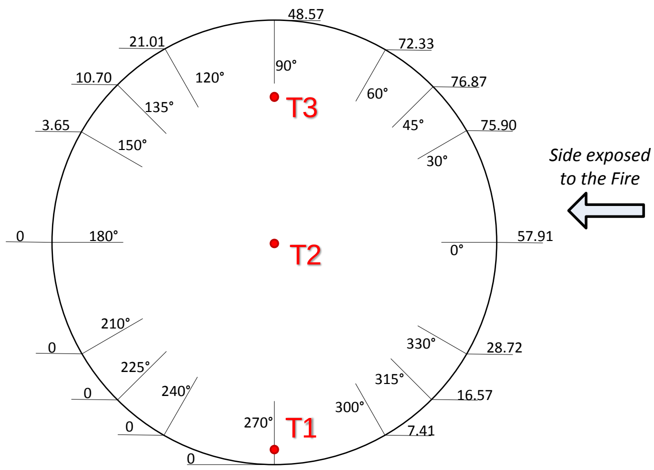

Figure 2: Schematization of flux heat incident on the wall of tank V2. Tank diameter is 3m. Heat flux is reported in kW/m^2.

4. Results and discussion

Figure 3 shows the results obtained in the analysis of case–study “a”, where a high filling level (90%) was considered. Figure 3a shows the liquid temperature distribution at the beginning of the fire exposure, indicating that natural convection starts from the side exposed to the flame. The liquid near the hot wall moves upwards to the liquid–vapour interface and subsequently spreads towards the opposite side, moving then to the bottom. The flow field is also shown in Figure 3b, where vectors colour scale represents the magnitude of the axial velocity. At the beginning of the fire exposure an altered thermally liquid layer is not present, but the lading temperature is relatively homogeneous over all the liquid region and ranges between 296 and 300 K, while the ascent velocity is about of 0.5 m/s. The liquid thermal stratification begins to form after 100 s. Figure 3c shows the formation of a thin layer of about 4 cm near to the liquid–vapour interface. The convective motion and recirculation phenomena are also significant. The stratification is pronounced approaching the PRV (pressure relief device) set pressure (see Figure 3e), with the liquid bulk temperature ranging between 298 and 305 K. The axial velocity is weaker that that observed initially (Figure 3f) as the fluid is more stable from the thermodynamic point of view.

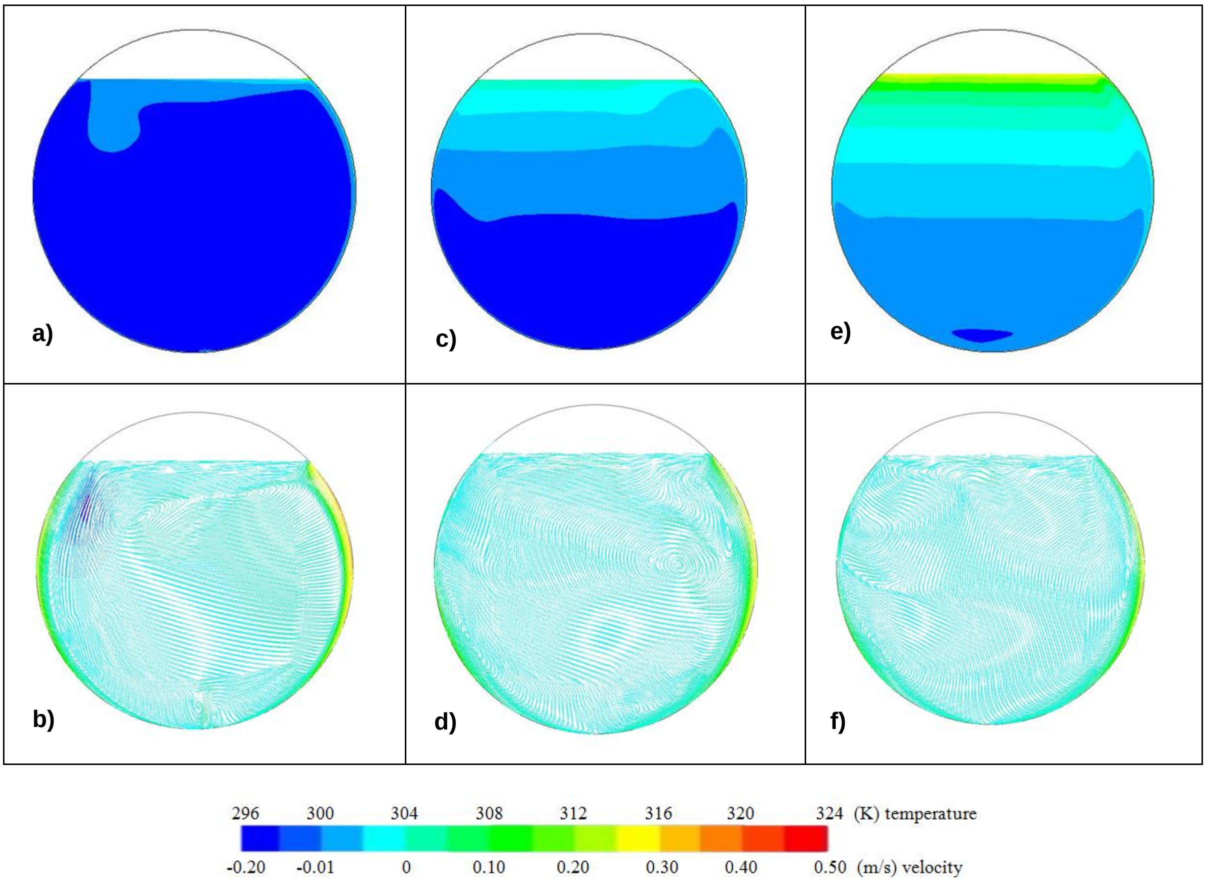

Figure 3: Results for case "a": temperature distribution (K) at 20 s (a), 100 s (c) and 200 s (e); velocity vectors coloured by axial velocity (m/s) at 20 s (b), 100 s (d) and 200 s (f). PRV opening time is 229.5 s.

Figure 4 shows the results obtained for case–study "b", where a lower filling level (70%) is considered. At the begin of the exposure, results are similar to the case–study "a". The stratified layer is absent and the axial velocities are similar with an ascent velocity of about of 0.5 m/s. Liquid stratification is more pronounced after 150 s since fire exposure. Figure 4c shows the presence of a hot layer of about 15 cm with a temperature between 305 and 310 K and a temperature gradient of about 60 K/m. The liquid bulk is cold (temperature ranging between 296 and 300 K) and an extremely lower temperature gradient is present with respect to the upper part of the tank (about 4 K/m). As shown in Figure 4e, a more homogeneous temperature distribution is present all over the liquid phase (overall temperature gradient is ranging between 5 and 20 K/m). Then, the liquid stratification is less pronounced with respect to the case–study "a". Moreover, in this case, due the lower filling level, the PRV opening time is reached after 336.5 s, that is 30% higher than the time required in case–study "a".

The dynamic liquid temperature profile at the three different spatial positions shown in Figure 2 and the internal pressure profile are shown in Figure 5 for both cases. The dynamic pressure behaviour is characterized by an irregular growth. For case "a" (see Figure 5a) at time larger than 150 s we observe a significant change in the slope of the pressure due to a more pronounced thermal stratification. The PRV opening time is reached after 229.5 s since fire exposure.

For case "b" (see Figure 5b), a gradual and slower vessel pressurization is obtained and then PRV opening time is much higher than in the other case (336.5 s). In fact, as shown in Figure 4, the stratification is less pronounced than in the case "a" and the temperature gradient is more homogeneous. This is also confirmed by the temperature values in three different positions for time a little lower than PRV opening time. In case–study "b", temperatures on the bottom vessel and in the liquid bulk are higher than temperatures obtained in the other case (of about 4 K), while in the proximity of the liquid–vapour interface, the two values are almost equal, as logical.

One of the advantages of the present modelling approach with respect to previous literature studies (Bi et al., 2011) is that the liquid phase may be tracked in detail, determining the thermal expansion. The transient liquid displacement due to thermal expansion is shown in Figure 6, in which a higher level rise is predicted for case “b” with respect to “case “a”.

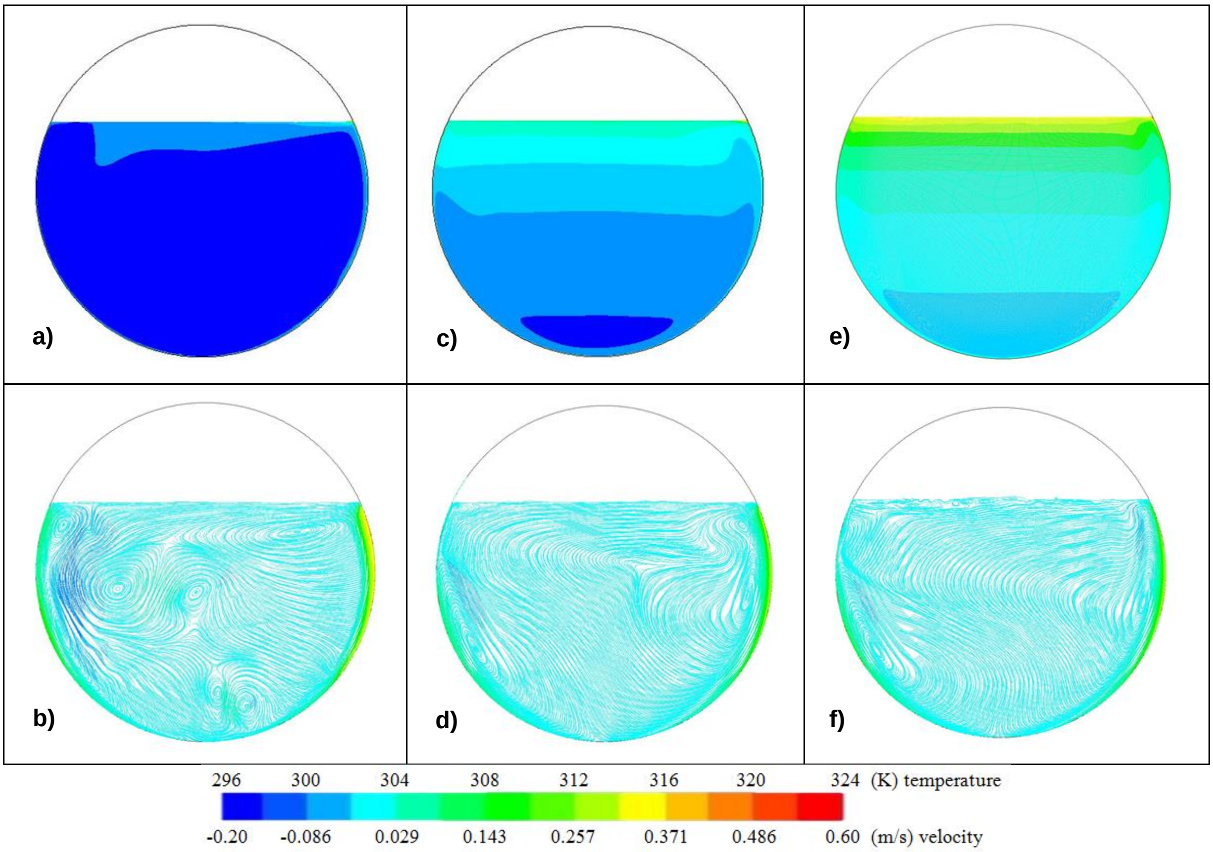

Figure 4: Results for case “b”: temperature distribution (K) at 30 s (a), 150 s (c) and 300 s (e); velocity vectors coloured by axial velocity (m/s) at 30 s (b), 150 s (d) and 300 s (f). PRV opening time is 336.5 s.

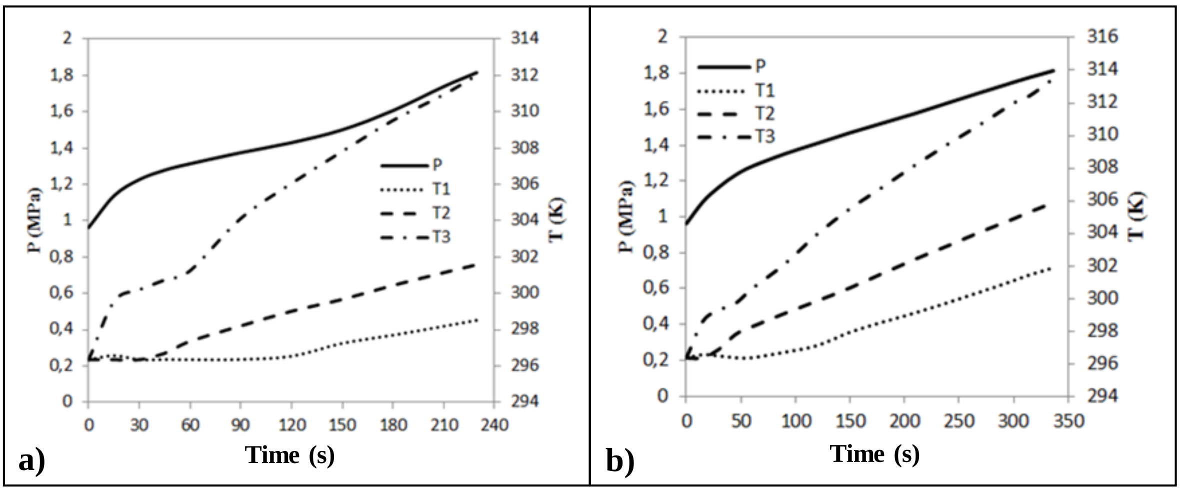

Figure 5: Pressure profile and liquid temperature profile (T1. near to bottom vessel, T2. in the liquid bulk, T3. near to liquid–vapour interface, see Figure 2) for: a) case “a”; b) case “b”.

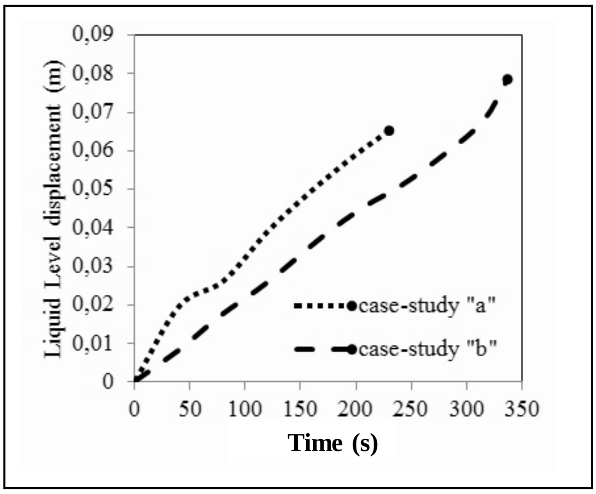

Figure 6: Comparison between the liquid thermal expansion predicted for case "a" and "b", in terms of liquid level rise (m).

5. Conclusions

In the present study, a CFD model of pressurized vessels exposed to an accidental fire, was developed, with the aim to determine the transient behaviour of the stored fluid during the heat-up. The model was coupled with conventional integral models for consequence assessment, that provided non-uniform heat flux boundary conditions. The use of a fine and rather uniform mesh, with refinements just near the walls, allowed evaluating the liquid level rise and considering any filling levels without a thickening in the proximity of liquid–vapour interface. In addition, cell distortions are absent and then, considering the single cell, the calculation is lighter than of other types of meshes, without any convergence problem. However, the high number of cells led to a high computational time. Detailed temperature and pressure predictions allowed obtaining key indications for the evaluation of the residual vessel resistance during fire exposure, e.g. the time to failure (Birk, 2012).
The present work constitutes a first attempt to consider the non-uniformity of fire exposition on a pressurized tank; in future, such model will be improved by taking into account the presence of solid walls and thus conjugate heat transfer effects.

Reference

Argenti, F., Landucci, G., Antonioni, G., Cozzani, V., 2014, Frequency evaluation for domino scenarios triggered by heat radiation exposure, Chem. Eng. Trans. 36, 373–378. doi:10.3303/CET1436063

Bi, M.S., Ren, J.J., Zhao, B., Che, W., 2011, Effect of fire engulfment on thermal response of LPG tanks, J. Hazard. Mater. 192, 874–879.

Birk, A.M., 2012, Scale considerations for fire testing of pressure vessels used for dangerous goods transportation, J. Loss Prev. Process Ind. 25, 623–630.

Birk, A.M., Cunningham, M.H., 1996, Liquid temperature stratification and its effect on BLEVEs and their hazards, J. Hazard. Mater. 48, 219–237.

D'Aulisa, A., Tugnoli, A., Cozzani, V., Landucci, G., Birk, A.M., 2014a, CFD modeling of LPG vessels under fire exposure conditions, AIChE J. 60, 4292–4305.

D'Aulisa, A., Simone, D., Landucci, G., Tugnoli, A., Cozzani, V., Birk, M., 2014b, Numerical simulation of tanks containing pressurized gas exposed to accidental fires: Evaluation of the transient heat-up, Chem. Eng. Trans. 36, 241–246. doi:10.3303/CET1436041

Landucci, G., D'Aulisa, A., Tugnoli, A., Cozzani, V., Birk, A.M., 2016, Modeling heat transfer and pressure build-up in LPG vessels exposed to fires, Int. J. Therm. Sci. 104, 228–244.

Lee, W., 1980, A pressure iteration scheme for two-phase ow modeling, in: Veziroglu, T.N. (Ed.), Multi-Phase Transport Fundamentals, Reactor Safety, Applications, Hemisphere Publishing, Washington DC.

Moodie, K., 1988, Experiments and modelling: An overview with particular reference to fire engulfment, J. Hazard. Mater. 20, 149–175.

Necci, A., Cozzani, V., Spadoni, G., Khan, F., 2015, Assessment of domino effect: State of the art and research Needs, Reliab. Eng. Syst. Saf. 143, 3–18.

Van Den Bosh, C.J.H., Weterings, R.A.P.M., 2005, Methods for the calculation of physical effects (Yellow Book), third. ed. Committee for the Prevention of Disasters, the Hague (NL).